A transposable element insertion in *IAA16* interrupts normal splicing and generates a novel dicamba resistance allele in *Bassia scoparia*

Jacob S Montgomery[1], Neeta Soni[1], Sofia Marques Hill[1], Sarah Morran[1], Eric L Patterson[1], Seth A Edwards[2,3], Sandaruwan Ratnayake[2], Yu-Hung Hung[2], Pratheek H Pandesha[2,4], R. Keith Slotkin[2,3], Franck Dayan[1], Todd Gaines[1]

[1]Department of Agricultural Biology, Colorado State University, Fort Collins, Colorado, USA.

[2]Donald Danforth Plant Science Center, St Louis, Missouri, USA.

[3]Division of Biological Sciences, University of Missouri, Columbia, Missouri, USA

[4]Division of Biology & Biomedical Sciences, Washington University in St. Louis, St Louis, Missouri, USA

Author for correspondence: Todd Gaines, Associate Professor, Colorado State University, 1177 Campus Delivery, Fort Collins, CO 80523, USA. (Email: todd.gaines@colostate.edu)

Keywords: Herbicide Resistance, Auxin, Evolution, Genetic Mapping, Transposable Elements, Weed Science

Summary

A dicamba-resistant population of kochia (*Bassia scoparia*) previously identified in Colorado, USA in 2012 was used to generate a synthetic mapping population that segregated simply for dicamba resistance. Linkage mapping to associate injury following dicamba application with genotype information from restriction-site-associated DNA sequencing identified a single locus in the kochia genome associated with resistance on chromosome 4. A mutant version of *Auxin/Indole-3-Acetic Acid 16* (*AUX/IAA16*; a gene previously implicated in dicamba resistance in kochia) is found near the middle of this locus in resistant plants. Long read sequencing of resistant plants identified a recently inserted Ty1/Copia retrotransposon near the beginning of exon two of *AUX/IAA16*, leading to interruption of normal splicing. Stable transgenic lines of *Arabidopsis thaliana* ectopically expressing the mutant and wildtype alleles of *AUX/IAA16* were developed. *Arabidopsis thaliana* plants expressing the mutant *AUX/IAA16* allele grew shorter roots on control media but had less reduction in root growth on media containing either dicamba (5 μM) or IAA (0.5 μM) compared to non-transgenic plants or those expressing the wildtype allele of *AUX/IAA16.* Protein modeling suggests the substitution of a specific glycine residue in the degron domain of AUX/IAA16 is especially important for resistance. A fitness cost associated with the mutant allele of *AUX/IAA16* has implications for resistance evolution and management of kochia populations with this resistance mechanism. We report a molecular assay for rapid detection of the mutant *AUX/IAA16* allele that can inform in-season management decisions of agricultural producers.

Significance

Synthetic auxin herbicides are amongst the most important herbicides in modern agriculture. Evolution of weeds that are resistant to these herbicides threatens sustainable crop production.

Understanding the basis of auxin herbicide resistance informs the development of improved weed control technologies. Additionally, auxin-resistant mutations and their pleotropic effects help us understand the role and function of natural and synthetic auxins. Here, we present the first report of a transposable element insertion within an herbicide target site gene leading to resistance and show that differential splicing leads to an adaptive allele. Our report advances the fields of auxin biology, weed management, and genome evolution.

Introduction

Weed control in modern agricultural production systems largely rely on the application of herbicides. The first synthetic herbicides to be commercialized (like 2,4-D; described by Quastel, 1950) were eventually determined to mimic the endogenous plant hormone auxin. The low cost of these synthetic auxin herbicides matched with their ability to selectively control broadleaf weeds in cereal production settings led to rapid adoption of spray-based weed management strategies. As new herbicides were discovered and commercialized, mixing multiple herbicides in a single spray mixture allowed for robust control of many of the most important weeds in diverse agricultural settings. While evolution of herbicide resistant weed populations has reduced the efficacy of many herbicides, evolution of resistance to synthetic auxin herbicides has been relatively slower and less frequent than other modes of action (Busi et al., 2018; Heap, 2024). Thus, some of the oldest herbicides (e.g., 2,4-D and dicamba) remain some of the most widely used across many agricultural settings. In fact, synthetic auxin resistance traits for dicot crops were developed and recently commercialized to provide producers more options to control weed populations that had evolved glyphosate resistance (Behrens et al., 2007; Wright et al., 2010). These two traits expanded the potential use cases and value of two of the most used synthetic

68 auxin herbicides, dicamba and 2,4-D. This expansion in use for these two herbicides has had the
69 unintended effect of increasing selection pressure for resistance alleles and has correlated with a
70 recent increase in the number of resistance reports to these herbicides. Beyond weed control,
71 these synthetic auxin compounds have been crucial for experiments to understand auxin
72 perception and signaling, perhaps the most complex of all plant signaling pathways (Ma et al.,
73 2017).

74 While the physiological mechanism of action for many herbicides have been well understood
75 for decades, the cascade of cellular responses following the application of a synthetic auxin
76 herbicide is convoluted and is the subject of many recent studies. The topic has been reviewed
77 several times, with new experimental results incrementally advancing our knowledge of the key
78 factors leading to plant death (Grossmann, 2010; Song, 2014; Christoffoleti et al., 2015;
79 McCauley et al., 2020). Auxin, whether synthetic or natural, first binds to one of the isoforms of
80 Transport Inhibitor Response 1/Auxin-Signaling F-Box (TIR1/AFB) (Dharmasiri et al., 2005;
81 Kepinski & Leyser, 2005). Once bound to TIR1/AFB, auxin acts as a "molecular glue",
82 mediating the interaction between TIR1/AFB and Auxin/Indole-3-Acetic Acid (Aux/IAA)
83 proteins. Identification of conserved domains and experimentation have produced a list of
84 residues in TIR1/AFB and Aux/IAA that are vital for this interaction (Tan et al., 2007; Uzunova
85 et al., 2016; Ramans-Harborough et al., 2023). This interaction leads to the ubiquitination and
86 eventual degradation of Aux/IAA proteins (Gray et al., 2001; Zenser et al., 2001). Because
87 Aux/IAA proteins act as transcriptional repressors of auxin response factor (ARF) proteins,
88 Aux/IAA degradation leads to the modulation of auxin-responsive gene expression (Grossmann,
89 2010). TIR1/AFB and Aux/IAA each have several orthologs, allowing for diversification for
90 different isoforms. For example, LeClere et al. (2018) show that Aux/IAA16 preferentially binds

with TIR1 and AFB6 (a homolog of AFB found in members of amaranthaceae, but not brassicaceae) in the presence of some auxin analogs, but not others. Different synthetic auxin herbicides likely promote the interaction of certain Aux/IAA proteins with certain TIR1/AFB proteins more efficiently, but this network of interactions is still not well understood.

A disruption in any step of this auxin signaling system (e.g. TIR1 binding auxin, Aux/IAA interacting with TIR1/AFB, or the ubiquitination and degradation pathway of Aux/IAA) could cause reduced activity of synthetic auxin herbicides (Ruegger et al., 1998; LeClere et al., 2018; Todd et al., 2020). Thus, evolution of synthetic auxin resistance should be relatively simple and common across weed species in the face of incredibly pervasive and strong selection pressure. However, mutants causing resistance to synthetic auxin herbicides often also cause a reduction in fitness compared to the wildtype (Roux & Reboud, 2005; Wu et al., 2021). While many auxin resistance alleles have likely evolved in many species, these alleles were likely rapidly purged during temporal pauses in management-induced selection for those alleles (i.e., if synthetic auxin herbicides were not used for several generations). Nevertheless, there are several reported cases of synthetic auxin herbicide resistance evolving and becoming widespread in weed species. Interestingly, all but one of these reports that specify a specific genetic basis (de Figueiredo et al., 2022a) pertain to mutations in or near the degron domain of Aux/IAA genes. LeClere et al. (2018) and Ghanizadeh et al. (2024) report, in closely related species, different mutations of a specific glycine residue in AUX/IAA16 that is known to be vital to normal auxin signaling. In an unrelated species, de Figueiredo et al. (2022b) report a 27-bp deletion that shortens the distance between the degron and PB1 domains of IAA2.

Here, we seek to understand the genetic and molecular basis of dicamba resistance in a population of kochia (*Bassia scoparia*) collected from Colorado, USA. We use linkage mapping

114 in a population segregating for resistance to identify a region of the genome that segregates with
115 resistance and contains a mutant version of *AUX/IAA16*. Long read sequencing allowed us to
116 identify a transposable element insertion in the coding region of *AUX/IAA16* that disrupts normal
117 splicing and changes several amino acids in the protein product relative to the wildtype. Ectopic
118 expression in *Arabidopsis thaliana* proves this mutant *AUX/IAA16* is sufficient to cause
119 resistance to dicamba, and protein modeling points to the importance of a glycine-to-threonine
120 substitution in the degron domain. We finish with a discussion of a fitness cost associated with
121 dicamba resistance and implications towards agricultural management of dicamba-resistant weed
122 populations.
123

124 **Results and Discussion**

125 *Characterization of herbicide resistance*

126 Dose response experiments were conducted to confirm and quantify the level of dicamba and
127 2,4-D resistance in a population of kochia (named M32) collected from Akron, Colorado, USA
128 (Figure 1A and 1B). Parameter estimates for two-parameter log-logistic models for each
129 population used in this experiment are shown in Table S1 and Table S2. In the dicamba
130 experiment, populations M32 and 9425 (a known dicamba-resistant kochia population previously
131 characterized by LeClere et al. (2018) and Pettinga et al. (2018)) had ED50 estimates 7.6
132 ($p<0.0001$) and 10.5 ($p<0.0001$) times greater than an herbicide-sensitive kochia population
133 (7710). The ED50 parameter represents the dose of dicamba needed to cause 50% injury to that
134 specific population. These estimates were significantly different from the herbicide-sensitive
135 control and from each other ($p<0.0001$), indicating dicamba resistance in M32 is not as high as in
136 9425. Nevertheless, the ED50 estimate for both resistant populations were greater than the

137 recommended field rate of dicamba (560g ha^{-1}), suggesting both populations would not be
138 controlled by dicamba in a field setting. Similarly, in the 2,4-D experiment, the ED50 estimate
139 for M32 was 5.0 ($p<0.0001$) times greater than that of the herbicide-sensitive control and greater
140 than the recommended field rate for 2,4-D.

141 While herbicide-sensitive plants show epinasty starting approximately 5 days after treatment
142 with dicamba or 2,4-D, resistant plants in our study do not show symptoms at all when treated
143 with a field rate of either herbicide. This lack of initial injury suggests that resistant plants either
144 rapidly metabolize/sequester the herbicides before they cause injury (Behrens et al., 2007; Ge et
145 al., 2010) or possess mutant target site(s) that reduce their interaction with their molecular
146 target(s) (Walsh et al., 2006; LeClere et al., 2018; de Figueiredo et al., 2022b). However, in
147 documented cases of metabolic auxin herbicide resistance, resistant plants do show symptoms of
148 herbicide damage but eventually recover (de Figueiredo et al., 2022a; Todd et al., 2024). It is true
149 that highly efficient metabolism genes from bacteria protects plants from herbicide-induced
150 symptoms (Behrens et al., 2007; Wright et al., 2010), but that has not been the case for weeds
151 with evolved auxin herbicide resistance.

152 To understand if physiological mechanisms keep dicamba from being absorbed or
153 translocated within resistant plants, radiolabeled dicamba was used to track its movement in
154 dicamba-resistant and -sensitive plants. Significantly less dicamba was absorbed by herbicide-
155 sensitive plants over 192 h compared to the two resistant populations, but rate of absorption
156 (time required for 90% absorption) was not significantly different between populations (Figure
157 1C, Table S3). Therefore, reduced dicamba absorption is not responsible for resistance. Time
158 series data for the translocation of radiolabeled dicamba out of the treated leaf did not fit well to
159 any tested models, so t-tests were used to determine if means differed between resistant and

160 sensitive populations at each time point (Figure 1D). Dicamba-resistant plants translocated less
161 dicamba out of the treated leaf compared to the sensitive plants. These results suggest that the
162 dicamba resistance mechanism in the experimental population is physiologically similar to one
163 described by Pettinga et al. (2018) and LeClere et al. (2018) that is caused by a mutation in
164 *BsAUX/IAA16*.
165
166 *A single locus on chromosome 4 is associated with dicamba resistance*
167 A quantitative trait loci (QTL) mapping approach was taken to identify regions of the
168 genome associated with dicamba resistance. Segregating F_3 populations were developed from
169 multiple independent biparental crosses using a dicamba-resistant plant as the male parent and a
170 dicamba-sensitive plant as the female parent. We expected to find one dominant locus controlling
171 dicamba-resistance because the ratio of alive:dead F_3 plants following dicamba treatment at a
172 rate of 560 g ha^{-1} (200:85) did not significantly differ from 3:1 ($p = 0.06$). We hypothesize that
173 the over-abundance of dead (herbicide-sensitive) plants may be caused by a fitness penalty
174 associated with the dicamba resistance mechanism that reduces germination frequency (see
175 section on fitness cost below). A novel double-digest restriction site associate DNA sequencing
176 (ddRADseq) protocol was used to determine genotypes of 103 segregating F_3 plants for 1,592
177 variant loci across the genome. A genome scan associating this genotype information to visual
178 injury rating identified one significant QTL that peaks at 88 Mbp on chromosome 4 (Figure 2A).
179 This interval contains *BsAUX/IAA16* at 87.4 Mbp, a gene that is important for the signaling of
180 auxin and has been implicated in auxin herbicide resistance in kochia and a closely related
181 species (LeClere et al., 2018; Ghanizadeh et al., 2024). The genotype of *BsAUX/IAA16* within
182 this QTL of plants from an independent segregating F_3 line explained 43% of variation in visual

183 injury following dicamba treatment at 560 g ha^{-1} (Figure 2B). While survival at this rate of
184 dicamba may be dominant, visual injury is incompletely dominant (Figure 2B) with a calculated
185 degree of dominance of -0.58 (Falconer, 1964). This dominance has important implications for
186 the spread of herbicide resistance alleles. For instance, a dominant trait is likely to spread more
187 quickly throughout a population, but is less likely to be driven to fixation under selection
188 (Holmes et al., 2022).
189
190 *A transposable element insertion in BsIAA16 causes a change in exon splicing*
191 Sequencing transcripts of *BsAUX/IAA16* from plants homozygous for either either
192 parental allele of the QTL discovered on chromosome 4 revealed near identical translated protein
193 sequences except for the region around the degron domain (Figure 3B; Table S4). The degron of
194 *BsAUX/IAA16* is located near the splice junction of exons one and two (Figure 3A). To
195 understand the sequence of genomic DNA in and around *BsAUX/IAA16*, a plant homozygous for
196 the resistant parent allele of *BsAUX/IAA16* was used for PacBio HiFi sequencing. After *de novo*
197 assembly, we discovered a 3,466 bp insertion at the beginning of exon two of *BsAUX/IAA16*
198 (Figure 3A). The insertion disrupts splicing of *BsAUX/IAA16*, replacing 16 bases at the
199 beginning of exon two in the wildtype with the final 19 bases of the insertion in the mutant
200 (Figure 3A). The mutant allele will herein be reffered to as $BsAUX/IAA16_{Mut}$, while the wildtype
201 allele will be referred to as $BsAUX/IAA16_{WT}$. This results in the addition of one amino acid and
202 the replacement of four more in the final protein product (Figure 3B; Table S4). The new splice
203 sites contain canonical GT and AG motifs. This change includes a substitution of a glycine to
204 threonine at the N-terminal end of degron domain (Figure 3B; Table S4). LeClere et al. (2018)
205 showed that a substitution of this glycine to asparagine in BsAUX/IAA16 is sufficient for

206 dicamba resistance in kochia. Similarly, Ghanizadeh et al. (2024) associate a substitution of this
207 glycine to aspartic acid with dicamba resistance in *Chenopodium album*, a closely related
208 species. Finally, NMR experiments by Ramans-Harborough et al. (2023) show that this glycine is
209 involved in the interaction between IAA and TIR1. Given the demonstrated importance of this
210 glycine residue, we hypothesize that the glycine to threonine substitution is the major driver of
211 dicamba resistance. Protein modeling shows that the larger side group of threonine contacts the
212 surface of the TIR1 binding pocket and causes steric hindrance of the IAA/TIR1 interaction
213 (Figure 3C). The rest of the mutant residues are found outside of the binding pocket of TIR1 and
214 in a disordered domain; thus, they are unlikely to affect IAA/TIR1 interactions (Tan et al., 2007;
215 Ramans-Harborough et al., 2023).

216 The retrotransposon insertion in *BsAUX/IAA16*$_{Mut}$ has 5 bp target site duplications
217 flanking 429 bp long terminal repeats (LTRs), identifying it as a Class I LTR element. No protein
218 coding sequences were found within this insertion, suggesting this element is non-autonomous
219 and relies on another transposable element for transposition. In order to search for the
220 corresponding autonomous element, we aligned the insertion to the *de novo* assembly built from
221 a dicamba-resistant plant and the reference genome built from a herbicide-sensitive plant
222 identifies a near perfect match (99.3% identity) 1 Mbp away on chromosome 4 and another
223 match (97% identity) on chromosome 2 in both assemblies (Table S5). Because the site on
224 chromosome 4 is the most similar across the genome and retrotransposons use a "copy and
225 paste" mechanism of transposition, we hypothesize this to be the donor location for the
226 retrotransposon insertion into in *BsAUX/IAA16*$_{Mut}$. A maximum likelihood phylogenetic tree
227 supports this idea, as the chromosome 4 element sequences from both assemblies form a distinct
228 clade from those on chromosome 2 (Figure S2). When comparing the insertion in

229 *BsAUX/IAA16*$_{Mut}$ with its donor site on chromosome 4, there is one single nucleotide
230 polymorphism (SNP) and two single base pair insertions (Table S5). These insertions are found
231 in homopolymer runs of at least 9 bp and are likely artifacts of the sequencing technology
232 (Espinosa et al., 2024). Given the approximated rate of mutation in *Arabidopsis thaliana* of
233 7×10^{-9} base substitutions per site per generation (Ossowski et al., 2010), we estimate a new
234 single base substitution to be generated in either one of these 3,466 bp regions approximately
235 every ~20,000 generations. This estimation is is very crude, and the insertion is extremely young
236 in the context of evolutionary time. Future research using this insertion could be used to test the
237 canonical paradigm that weedy adaptation is the consequence of selection on standing genetic
238 variation versus the more contentious proposition that management-induced stress can generate
239 contemporary adaptive alleles in weeds (Dyer, 2018).

240 Since we had identified a likely donor retrotransposon and had not detected any protein
241 coding sequences within this element, there must have been an autonomous element which
242 retrotransposed the donor from chromosome 4 to *BsAUX/IAA16*$_{Mut}$. To identify the autonomous
243 version(s) of the retrotransposon within *Bs AUX/IAA16*$_{Mut}$, NCBI BLAST was first used to find
244 similar LTRs in the previously assembled reference genome (Hall et al., 2023). Putative LTRs
245 were first filtered by sequence similarity and distance between other putative LTRs. Matches
246 were only considered if the putative LTRs were in the same orientation. Once matches were
247 found, identification of required retrotransposon domains was performed for each match (see
248 methods). This process led to the identification of a single autonomous element that contained all
249 domains required for transposition (Table SX). This 13kb putative autonomous retrotransposon,
250 named gi_5_13kb, was found on chromosome 5 (Figure 4B). There are two known superfamilies
251 of retrotransposons, Ty1/Copia and Ty3/Gypsy. To determine which gi_5_13kb belongs, we first

252 built a curated list of all high-confidence LTR transposons in Arabidopsis which contained all
253 required domains. We accomplished this using a combination of RepetDBv2 and TESorter. Then,
254 we used the predicted amino acid sequence of these high-confidence LTR transposons to build a
255 phylogenetic tree with the predicted amino-acid sequence of gi_5_13kb. This element clustered
256 within the Ty1/Copia branch of the tree (Figure 4A). We have subsequently named this novel
257 Ty1/Copia element *Outlaw*. This one protein-coding version of the *Outlaw* seems to be driving
258 retrotransposition of the non-autonomous element that generated herbicide resistance in this
259 population of kochia.
260
261 *BsIAA16$_{Mut}$ expression is sufficient for dicamba resistance in Arabidopsis thaliana*
262 To demonstrate the role of *BsAUX/IAA16$_{Mut}$* in dicamba resistance, stable transgenic lines
263 of *Arabidopsis thaliana* expressing *BsAUX/IAA16$_{WT}$* or *BsAUX/IAA16$_{Mut}$* were generated through
264 the floral dip method. When seeds were grown on phytoagar plates without herbicide,
265 Arabidopsis expressing *BsAUX/IAA16$_{Mut}$* grew shorter roots compared to those expressing
266 *BsAUX/IAA16$_{WT}$* or with no transgene (Figure 5A). This is further evidence of a likely fitness
267 cost associated with disrupting normal auxin signaling in roots as seen by de Figueiredo et al.
268 (2022b) and LeClere et al. (2018). When grown on media containing 5 µM dicamba, only
269 seedlings expressing *BsAUX/IAA16$_{Mut}$* were able to grow and had significantly longer roots when
270 normalized to the length of roots grown on solvent-only media (Figure 5B). A similar result was
271 seen when seedlings were grown on media containing 0.5 µM IAA (Figure 5C), suggesting this
272 variant of AUX/IAA16 also reduces the perception of natural auxin. No seeds grew roots on
273 media containing 5 µM or 0.5 µM 2,4-D.

274 To confirm the results of root growth assays that indicate *BsAUX/IAA16*$_{Mut}$ is sufficient
275 for dicamba resistance, plants of select T_3 lines either expressing *BsAUX/IAA16*$_{WT}$,
276 *BsAUX/IAA16*$_{Mut}$, or no transgene were grown in the greenhouse and treated with 140 g dicamba
277 ha^{-1}. Only one of the lines expressing *BsAUX/IAA16*$_{Mut}$ showed less visual injury than the other
278 lines tested and appeared stunted and darker green than the other lines even when no dicamba
279 treatment was administered (Figure S3). Quantitative PCR indicated similar expression levels of
280 *BsAUX/IAA16* between lines expressing *BsAUX/IAA16*$_{WT}$ or *BsAUX/IAA16*$_{Mut}$ (Figure 5D).
281 However, plants expressing *BsAUX/IAA16*$_{Mut}$ had no detected induction of auxin response genes
282 *AtIAA19* or *AtGH3.3* six hours after dicamba treatment (Figure 5E and 5F). These genes are
283 known to have increased expression following exposure to natural or synthetic auxins (Tatematsu
284 et al., 2004; Gleason et al., 2011; de Figueiredo et al., 2022b). Differences between root and
285 whole plant assays may be caused by differences in expression of the transgene between root and
286 above ground tissue.
287
288 *The BsIAA16*$_{Mut}$ *allele is associated with a reduction in fitness*
289 Because we hypothesize this insertion interferes with natural auxin signaling as shown by
290 LeClere et al (2018) and de Figuieredo et al. (2022), we expect this change to also confer a
291 fitness penalty in the absence of synthetic auxin application. To formally test this, kochia plants
292 were grown from an F_3 family that is segregating for the *BsAUX/IAA16* locus and fitness traits
293 were measured without the application of auxin. The ratio of genotypes significantly differed
294 from the expected 1:2:1 ($p<0.0001$), with fewer than expected plants with the mutant
295 *BsAUX/IAA16* locus (Figure 6). All seedlings that emerged were used in the experiment, so we
296 hypothesize that *BsAUX/IAA16*$_{Mut}$ causes reduced germination. Further, *BsAUX/IAA16*$_{Mut}$ was

297 associated with shorter plants, both at transplanting and at maturity (Figure 6). Evidence of a
298 fitness cost associated with herbicide resistance has implications on kochia management. For
299 instance, if dicamba is not used for several years, the frequency of *BsAUX/IAA16*$_{Mut}$ is expected
300 to decrease. High gene flow in kochia facilitates rapid spreading of alleles across long distances
301 and maintenance of high genetic diversity across the genome following selection of rare
302 herbicide resistance alleles (Martin et al., 2020; Ravet et al., 2021). The negative pleotropic
303 effect of *BsAUX/IAA16*$_{Mut}$ may help limit the expected spread of this resistance allele and allow
304 producers to better manage resistant populations that have already established.

305 Taken together, our results further emphasize the importance of the glycine residue within
306 the degron domain of AUX/IAA proteins in auxin signaling. They also reinforce the importance
307 of *BsAUX/IAA16*, specifically, in dicamba action. We describe the first instance of the insertion
308 of a mobile genetic element creating an herbicide resistance allele through gain-of-function.
309 These results highlight the amazing adaptability of weedy genomes, and the unlikely ways
310 genomes evolve in the face of strong selection pressures (Montgomery et al., 2024).
311

312 Experimental Procedures

313 *Plant growth and herbicide treatment conditions*

314 Unless otherwise noted, all plants were grown in greenhouses at Colorado State University in
315 3.8-cm by 3.8-cm by 5.8-cm pots containing fine-grade potting mix (Fafard #2-SV; American
316 Clay Works, Denver, CO). Temperatures were held between 22C and 24C, and supplemental
317 light was provided by liquid halogen grow lights to ensure a photoperiod of 14h/10h. Herbicide
318 applications were made using a moving overhead single-nozzle sprayer (DeVries Manufacturing,
319 Hollandale, MN) calibrated to deliver 187 L ha^{-1}. Engenia (BASF, Research Triangle Park, NC)

320 was used for dicamba applications, and Clean Amine (Loveland Products, Inc., Loveland, CO)
321 was used for 2,4-D applications. For kochia, herbicide applications took place when plants were
322 10-15 cm tall, and for Arabidopsis, plants were sprayed when they had 10-12 leaves and before
323 bolting.
324
325 *Plant material*
326 The M32 population of kochia was collected near Akron, Colorado as part of an herbicide
327 resistance survey conducted between 2012 and 2014 (Westra et al., 2019). Seeds from this field
328 collection were grown and the resulting plants were treated with 560 g dicamba ha^{-1}. Survivors
329 were open-pollinated, and their seed was combined to form a composite dicamba-resistant seed
330 lot. Approximately 50 seeds from this combined lot were grown and treated with 560 dicamba
331 ha^{-1}. The individual with the least herbicide injury was used as a male parent in a biparental cross
332 with an individual from the population 7710, an inbred, herbicide-susceptible population
333 (Preston et al., 2009) that was used to generate the first reference genome assembly for kochia
334 (Patterson et al., 2019). To make the cross, immature flowers of the dicamba-sensitive plant were
335 emasculated using forceps under a microscope, and the emasculated flowers were labeled. The
336 two plants were then grown to maturity together in a pollen-exclusion tent. Seeds from the
337 dicamba-sensitive plant were collected and grown; the resulting plants were treated with 560 g
338 dicamba ha^{-1}. A Kompetative Allele Specific PCR (KASP) assay that detects $BsAUX/IAA16_{Mut}$
339 was used to confirm survivors as hybrids (primer sequence and thermocycler conditions found in
340 Table S6). Several confirmed hybrid plants were grown in pollen exclusion tents and self-
341 pollinated to create several F_2 families. Plants from two F_2 families were grown, but because of

342 low seed production in the F_1 generation, plants were allowed to self-pollinate with no selection
343 to produce F_3 families.
344
345 *Dose response*
346 Plants were grown from the 7710 (Preston et al., 2009) and 9425 (LeClere et al., 2018)
347 populations as well as from the M32 composite resistant seed lot. Plants were treated with one of
348 several rates of dicamba. These rates included 0, 8.75, 17.5, 35, 70, 140, 280, 560, and 1120 g
349 dicamba ha^{-1} for the herbicide-sensitive population and 0, 70, 140, 280, 560, 1120, 2240, and
350 4480 g dicamba ha^{-1} for the herbicide-resistant populations. Six uniform plants were used for
351 each population at each herbicide rate before being returned to the greenhouse. Visual injury and
352 survival were rated 21 days after treatment (DAT). The drc package (v3.0-1; (Ritz et al., 2015))
353 in R (v4.0.2; (R-Core-Team, 2021)) was used to fit the injury data to a 2-parameter log-logistic
354 dose response curve. Significant difference is in the ED50 parameter were determined using the
355 compParm function from the drc package (Ritz et al., 2015).
356
357 *Herbicide absorption and translocation profiles*
358 Kochia plants from M32, 7710, and 9425 were germinated in a growth chamber (60%
359 relative humidity, 21/18 C, and 16/8 h photoperiod) in potting soil and transplanted to fine sand
360 when they reached ~3 true leaves. The plants were irrigated with fertilizer until the plants
361 reached 10 cm in height. At this point, aluminum foil was used to cover the second youngest
362 fully expanded leaf while the plants were sprayed with 560 g dicamba ha^{-1}. After spraying, the
363 aluminum foil was removed, the leaf was then marked and treated with 10 μL of a ^{14}C-labeled
364 dicamba solution (total radioactivity of 3.33 KBq or 200,000 dpm per plant). Plants were

365 returned to the growth chamber until sampling at 3, 6, 12, 24, 48, 96, and 192 h after treatment.
366 The treated leaf, remaining above ground tissue, and below ground tissue of three biological
367 replicates were separated for each population at each time point. The treated leaf was washed in
368 10 mL 10% methanol + 1% NIS, and radioactivity in this wash solution was quantified in 10 mL
369 of scintillation mixture (Ecoscint XR, National Diagnostics, Atlanta, GA) using liquid
370 scintillation spectrometry (Packard Tricarb 2300TR, Packard Instrument Co., Meriden, CT).
371 Plant tissue was dried in an oven at 60 C for at least 14 d before oxidation in a biological
372 oxidizer (OX500; RJ Harvey Instrument Co., Tappan, NY) followed by radioactivity
373 measurement by liquid scintillation spectrometry. Absorption time series data was fitted to a
374 rectangular hyperbolic model, and the parameters "absorption max" (*Amax*) and "time to 90
375 percent absorption" (*t90*) were estimated and compared in R (Kniss et al., 2011; Ritz et al., 2015;
376 R-Core-Team, 2021). Because the time series data for translocation of dicamba outside of the
377 treated leaf did not fit any of the models proposed by Kniss et al. (2011), t-tests were used to
378 determine if the amount of dicamba retained in the treated leaf was different between dicamba-
379 resistant and dicamba-sensitive populations at each time point.
380
381 *QTL mapping*
382 Plants from several F_3 families derived from a biparental cross described above were grown
383 and treated with 560 g dicamba ha^{-1}. Two families that segregated for survival following dicamba
384 treatment (4-1-1 and 4-5-10, each from a different F_1 hybridization event) were used for QTL
385 mapping. Approximately 150 plants from the F_3 family 4-5-10 were grown, and a single young
386 leaf was sampled and frozen in liquid nitrogen before treatment with 560 g dicamba ha^{-1}. Visual
387 injury was rated for each plant 21 DAT, and DNA was extracted from each plant (including the

388 original parents of the cross) using the CTAB method (Doyle & Doyle, 1990). The concentration
389 of each DNA sample was quantified using the Qubit™ dsDNA BR kit (Thermo Scientific,
390 Waltham, MA) and diluted to 20 ng/µl. A double-digest restriction-site associated DNA
391 sequencing (ddRADseq) protocol was developed in conjunction with the University of
392 Minnesota Genomics Center (Minneapolis, MN) by estimating the number of RAD sites across
393 the reference genome (Patterson et al., 2019) for several enzyme combinations and then
394 empirically testing the BtgI-TaqI combination on several samples at multiple sequencing depths.
395 DNA from the two original parents and 103 plants from the 4-5-10 F_3 family were used for
396 ddRADseq with BtgI and TaqI as the restriction enzymes with a target of 4 million 150 bp single
397 end reads per sample. Library prep and sequencing was completed by the University of
398 Minnesota Genomics Center.
399 Reads from each sample were passed through a variant calling pipeline that can be found at
400 github.com/JMont12/dicamba_kochia. Briefly, raw reads were trimmed with Trimmomatic
401 (v0.36; (Bolger et al., 2014)) and aligned to the reference genome of kochia (Hall et al., 2023)
402 using the burrows-wheeler aligner (v0.7.17, (Li & Durbin, 2009)). The alignments were
403 processed with samtools (v1.15, (Li et al., 2009)) and passed to GATK (v4.2.0, (Poplin et al.,
404 2018; Van der Auwera & O'Connor, 2020)) to call variants and filter them based on depth,
405 quality, and strand bias. Variants were further filtered using custom scripts to only include
406 biallelic single nucleotide polymorphisms that were homozygous and different between the two
407 original parents. Filtered variants and phenotype data were used to conduct a genome scan within
408 the qtl2 package in R (v0.32, (Broman et al., 2019)). Because a permutation test for significance
409 was not possible, a significance threshold was established through a Bonferroni correction of
410 alpha=0.05 considering the number of tests to equal the number of filtered markers used in the

411 scan then converting the adjusted p-value to LOD as described by Nyholt (2000). The genotype
412 around the QTL discovered on chr4 was determined for 210 plants from another F_3 family (4-1-
413 1) using the KASP assay developed for the *BsAUX/IAA16* gene (primer sequence and
414 thermocycler conditions in Table S6). A simple linear model was fitted using visual injury 21
415 DAT as the dependent variable and *BsAUX/IAA16* genotype as the independent variable and
416 plotted using ggplot2 (v3.4.4, (Wickham, 2016)) in R (R-Core-Team, 2021).
417
418 *$BsIAA16_{M32}$ sequencing*
419 Total RNA was extracted using the Direct-zol RNA Microprep kit (Zymo Research, Irvine,
420 CA) from individuals of the 4-5-10 selected line that were homozygous for either parental allele
421 of *BsAUX/IAA16* based on the results of KASP testing. This RNA was used to generate cDNA
422 libraries for each sample using the ProtoScript® II First Strand cDNA Synthesis Kit (New
423 England Biolabs, Ipswich, MA). Primers that bind to the beginning and end of the *BsAUX/IAA16*
424 gene (Table S7) were used with the EconoTaq PLUS Green kit (LGC, Teddington, Middlesex,
425 UK) to amplify the full-length coding sequence. The product of each PCR reaction was run on a
426 1% agarose gel to ensure a single product, then sent to Azenta (Burlington, MA) for Sanger
427 sequencing using the forward and reverse primers.
428 To determine the genomic sequence around the $BsAUX/IAA16_{Mut}$, 2 g of dark-treated leaf
429 tissue from a plant that was homozygous for $BsAUX/IAA16_{Mut}$ was sampled and flash frozen in
430 liquid nitrogen. This tissue was sent to Corteva Agriscience Center for Genome Excellence
431 (Johnston, IA) for whole genome PacBio HiFi sequencing to a depth of ~30X. The resulting
432 reads were assembled with HiFiasm (Cheng et al., 2021), and *BsAUX/IAA16* was located by
433 BLAST (Camacho et al., 2009).

434

435 *Characterization of transposable element insertion*

436 To find similar elements to the one inserted in *BsAUX/IAA16*$_{Mut}$, the sequence of the 429
437 bp LTRs of the insertion were aligned to the kochia 2.0 reference genome assembly (Hall et al.,
438 2023) and to the newly created assembly described above using BLAST (Camacho et al., 2009).
439 Sequential filtering was used to identify the autonomous version of the element. First, alignments
440 of >85% identity and >100bp alignment length were identified as putative LTRs. Next, only
441 putative LTRs that were between 25 kb and 4 kb apart and in the direct orientation were
442 considered potential *Outlaw* transposon family members. Finally, of the elements of the proper
443 length and LTR orientation, we then only considered putative elements that contained all
444 required retrotransposon domains as potential autonomous elements. Necessary retrotransposon
445 domains were identified manually and with TESorter (Zhang et al., 2022). Specifically, the
446 required domains that we used were as follows: gag, pol (RNAseH, Integrase, Protease, Reverse
447 Transcriptase), tRNA Primer Binding Site, and Polypurine Tract.

448

449 *Autonomous transposable element characterization*

450 To classify the retro element into one of two possible superfamilies (Ty1/Copia or Ty3/Gypsy),
451 we used the *Arabidopsis thaliana* transposable element annotation dataset from RepetDBv2
452 (Amselem et al., 2019). We procured all Ty1/Copia and Ty3/Gypsy nucleotide elements and
453 predicted the protein domain sequences from this dataset using TESorter (Zhang et al., 2022).
454 We only used TEs which had all required retrotransposon domains (both pol and gag). We then
455 manually concatenated all pol domain proteins (RT, RNaseH, Protease, Integrase) as a single
456 polypeptide for each transposable element and then used *Outlaw* predicted pol polypeptide

457 sequence to create a phylogenetic tree. MegaX was used to align all of the proteins using
458 MUSCLE to create a maximum likelihood tree with 500 bootstraps (Kumar et al., 2018).
459
460 *Development of transgenic Arabidopsis thaliana lines*
461 The coding sequence of *BsAUX/IAA16*$_{Mut}$ and *BsAUX/IAA16*$_{WT}$ were amplified from
462 cDNA libraries discussed above using the PrimeSTAR MAX DNA Polymerase kit (Takara Bio
463 USA, Inc., San Jose, CA) and primers with tails that complement restriction sites in the
464 expression vector *pFGC5941* (primer sequences and thermocycler conditions in Table S8).
465 Empty *pFGC5941* was digested with AscI and BamHI (New England Biolabs, Ipswich, MA),
466 and the *BsAUX/IAA16* amplicons were ligated into the digested vector using the In-Fusion
467 Cloning kit (Takara Bio USA, Inc., San Jose, CA). Plasmid sequencing ensured correct assembly
468 of expression vectors (Plasmidsaurus, Eugene, OR). Vectors containing *BsAUX/IAA16*$_{Mut}$ or
469 *BsAUX/IAA16*$_{WT}$ were transformed into the GV3101 strain of *Agrobacterium tumefaciens*, and
470 subsequently transfected into the Col-0 genotype of *Arabidopsis thaliana* using the floral dip
471 method (Clough & Bent, 1998). Transformants were selected by spraying T_1 seedlings with
472 BASTA herbicide (BASF, Research Triangle Park, NC) and confirmed with PCR for the
473 transgene (primers and thermocycler conditions found in Table S9). Confirmed transformants
474 were inbred for two generations, and T_3 populations fixed for the transgene were identified by
475 spraying seedlings with BASTA herbicide and PCR for the transgene.
476
477 *Effect of dicamba on transgenic Arabidopsis lines*
478 Seeds of Col-0 and of fixed T_3 lines of Arabidopsis, each from a different transformation
479 event, were gas sterilized and plated on media plates containing synthetic or natural auxin as

480 described by de Figueiredo et al. (2022b). Plates were incubated in a growth chamber with a
481 yellow light filter to prevent indole-3 acetic acid degradation. Ten seeds were used per
482 population for each treatment. Root growth was measured 7 d after moving plates to growing
483 conditions. T-tests were used to detect significant differences between lines expressing
484 *BsAUX/IAA16*$_{Mut}$ compared to the Col-0 control. Results were plotted with ggplot2 in R.
485 Plants from select T_3 lines were grown to the 10-leaf stage and either untreated or treated
486 with 140 g dicamba ha^{-1}. Four plants of each population were used for each treatment. Photos
487 were taken 21 DAT to illustrate visual injury. Young leaf tissue was collected from treated and
488 untreated plants 6 h after treatment. Total RNA was extracted from these leaf samples using the
489 Direct-zol RNA Microprep kit (Zymo Research, Irvine, CA), and cDNA libraries were generated
490 using the ProtoScript® II First Strand cDNA Synthesis Kit (New England Biolabs, Ipswich,
491 MA). Following the methods of de Figueiredo et al. (2022b), relative expression was quantified
492 for the *BsAUX/IAA16* transgene (primers and thermocycler conditions available in Table S10)
493 and the auxin response genes *AtIAA19* and *AtGH3.3* using *AtCyclophilin* as a reference gene.
494
495 *In silico mutagenesis of IAA variants*
496 The crystal structure of the degron of IAA7 bound to TIR1 in the presence of 2,4-D
497 (2p1n) was downloaded from the RCSB Protein Data Bank (Tan et al., 2007). Mutagenesis of the
498 G127 residue was conducted and visualized in PyMOL.
499
500 **Data Statement**

The RAD sequencing data from the segregating F3 line used in the mapping project and the PacBio HiFi sequencing used to generate the de novo genome assembly are being submitted to the NCBI SRA database and will be available upon publication.

Acknowledgments

This research was supported in part by BASF SE, by the Colorado Wheat Administrative Committee, and by the USDA National Institute of Food and Agriculture, Hatch project COL00783 to the Colorado State University Agricultural Experiment Station.

Figures

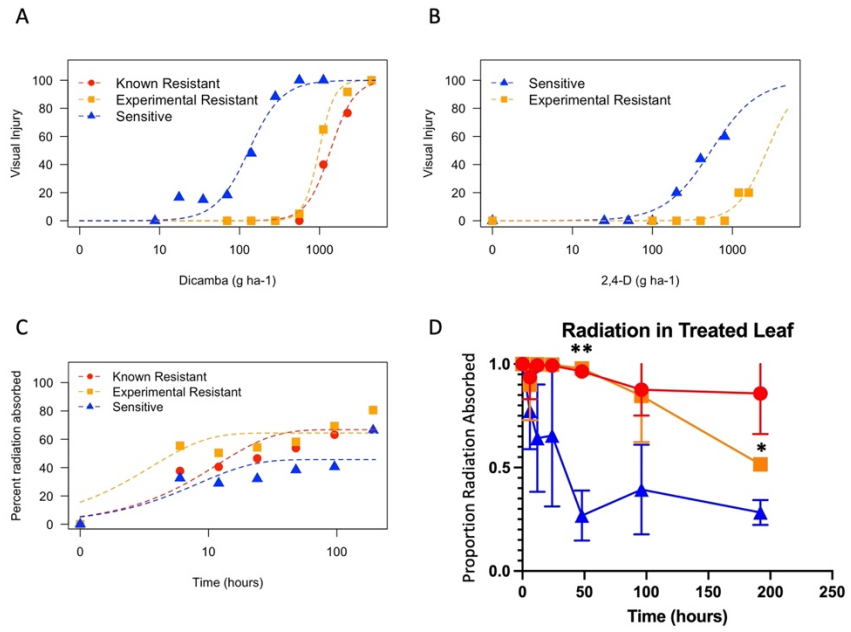

Figure 1. Dose response curves showing magnitude of resistance towards dicamba (A) and 2,4-D (B) for the M32 population of *Bassia scoparia* (Experimental Resistant) compared to a known dicamba-sensitive population and known dicamba-resistant population (LeClere et al., 2018;

515 Pettinga et al., 2018). C) Time course of ^{14}C dicamba absorption showing lack of herbicide
516 absorption is not associated with dicamba resistance in dicamba-resistant populations of *Bassia*
517 *scoparia*. D) Proportion of absorbed ^{14}C dicamba retained in the treated leaf showing less
518 dicamba exits the treated leaf in dicamba-resistant populations compared to a dicamba-sensitive
519 population. Error bars represent standard error. *=p<0.05, **=p<0.01. Populations are
520 represented by the same colors and symbols as in A-C.
521

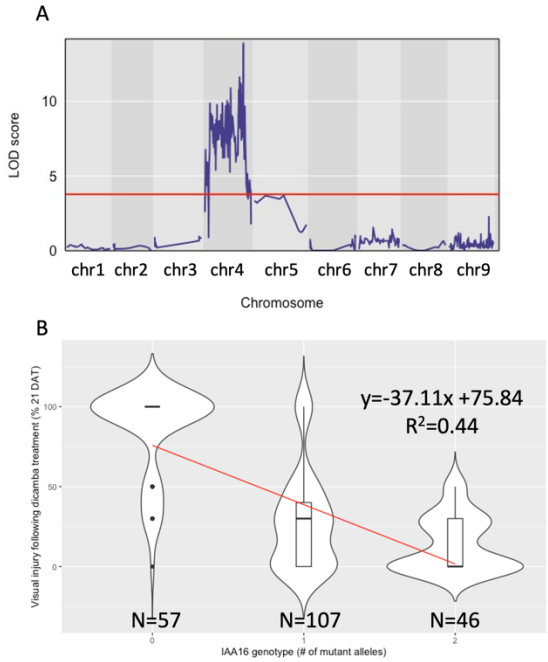

522

523 Figure 2. A) Quantitative trait loci (QTL) genome scan from a segregating F_3 population derived
524 from a biparental cross of herbicide-resistant and -sensitive *Bassia scoparia* plants. Red line
525 represents a significance threshold determined by Bonferroni-adjustment of alpha=0.05 followed
526 by conversion to LOD as described by Nyholt (2000). B) Violin plot displaying the effect of
527 *BsAUX/IAA16* genotype on visual injury in an independent segregating F_3 population of *Bassia*

scoparia. Red line represents a linear model fitted to all points with equation listed in black. Number of observations for each genotype listed at the base of the graph.

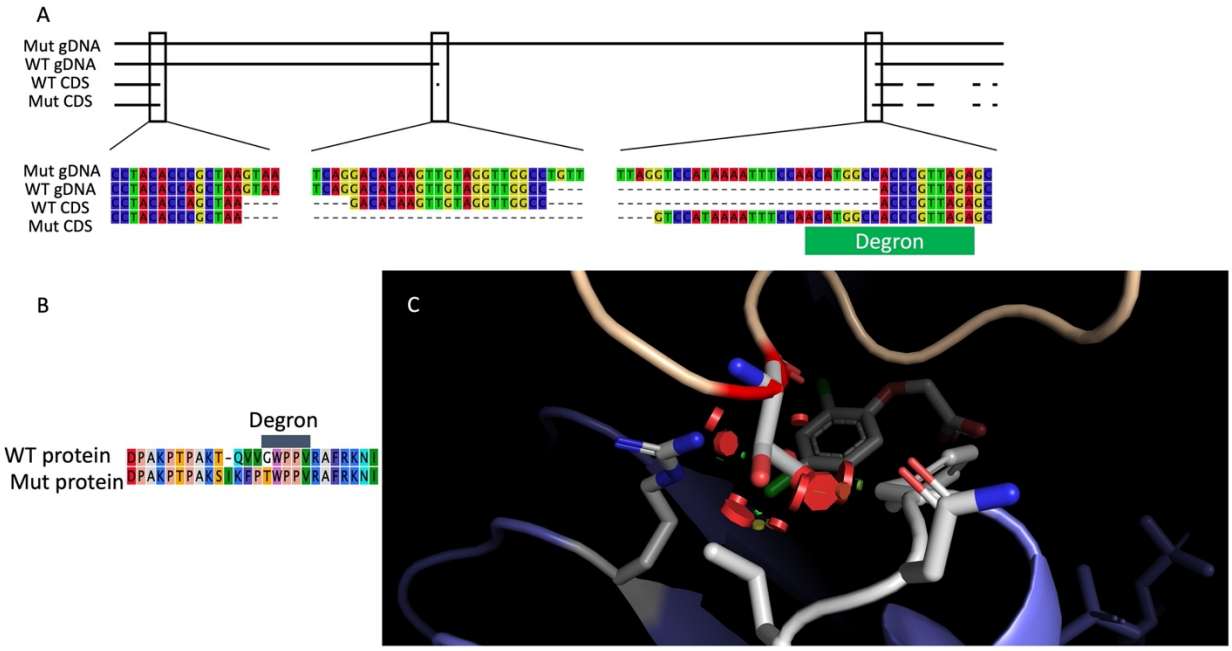

Figure 3. A) Genomic and coding sequence for *BsAUX/IAA16* alleles detected in a mapping population segregating for dicamba resistance. An insertion in the beginning of exon two of *BsAUX/IAA16* changes the coding sequence near the degron domain in the mutant allele. B) Amino acid sequence of mutant (Mut) and wildtype (WT) alleles of *BsAUX/IAA16* around the degron domain. C) Crystal structure of IAA7 (wheat) bound to TIR1 (slate) showing the glycine 127 residue (red) superimposed over the predicted structure if this residue is substituted for threonine, colored by element (carbon=grey, oxygen=red, nitrogen=blue, chlorine=green). Residues of TIR1 that are within 4Å of the threonine residue are colored by element, and 2,4-D is in the background, colored by element. Clashes are shown as red discs.

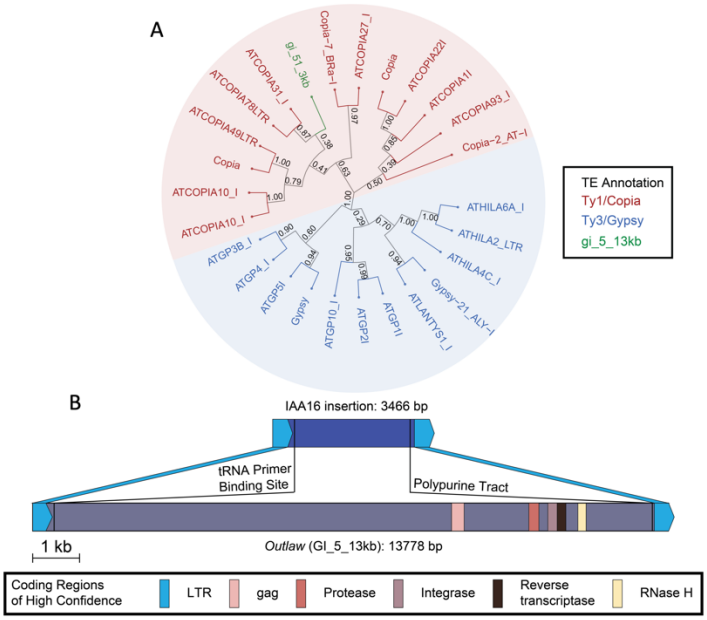

Figure 4. Characterization of autonomous element driving transposition of the retrotransposon that was inserted in *BsAUX/IAA16*. A) Maximum likelihood phylogenetic tree showing evolutionary relationships between autonomous LTR elements from Arabidopsis and the autonomous *Outlaw* element discovered in *Bassia scoparia*. B) comparison of nonautonomous (top) and autonomous (bottom) versions of *Outlaw*. Colored blocks represent regions necessary for retrotransposition.

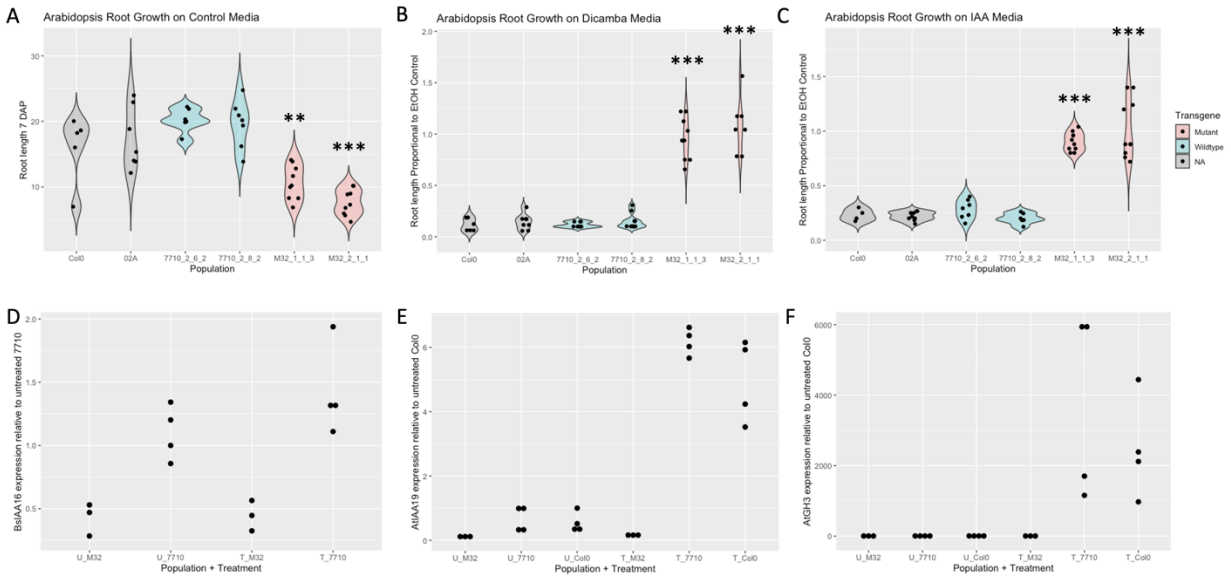

Figure 5. Root length of *Arabidopsis thaliana* plants expressing either $BsAUX/IAA16_{Mut}$ (populations starting in Mut), $BsIAA16_{WT}$ (populations starting in WT), or no transgene (Col0 and 02A) grown on phytoagar media. Proportional root length (compared to control) of the same populations when grown on media containing 5 µM dicamba (B) or 0.5 µM IAA (C). Expression of the *BsAUX/IAA16* transgene (D) and the auxin response genes *AtAUX/IAA19* (E) and *AtGH3.3* (F) in plants expressing $BsAUX/IAA16_{Mut}$ (M32), $BsAUX/IAA16_{WT}$ (7710), or no transgene (Col0) that were either treated (T) or untreated (U) with 140 g dicamba ha^{-1} six hours after treatment. Each observation is represented by a black dot.

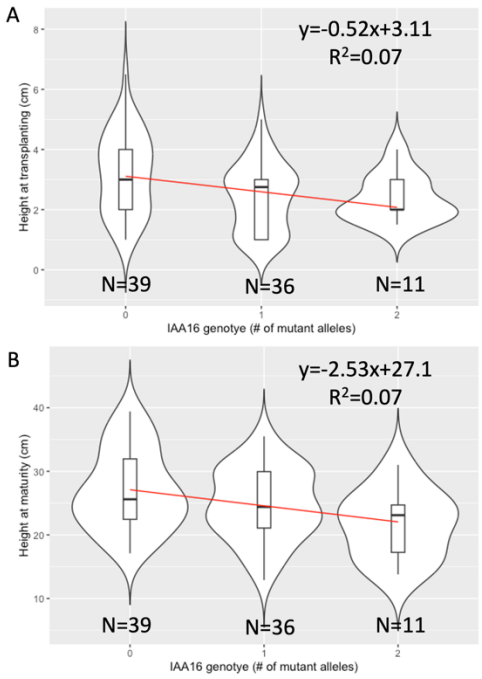

Figure 6. Effect of *BsAUX/IAA16* genotype on plant height either at transplanting (A) or maturity (B) of kochia plants from an F_3 population segregating for dicamba resistance.

569 **References**

570 Amselem, J., Cornut, G., Choisne, N., Alaux, M., Alfama-Depauw, F., Jamilloux, V. et al. (2019)
571 RepetDB: a unified resource for transposable element references. *Mob DNA*, **10**, 6.
572 Behrens, M.R., Mutlu, N., Chakraborty, S., Dumitru, R., Jiang, W.Z., Lavallee, B.J. et al. (2007)
573 Dicamba resistance: enlarging and preserving biotechnology-based weed management
574 strategies. *Science*, **316**, 1185-8.
575 Bolger, A.M., Lohse, M. & Usadel, B. (2014) Trimmomatic: a flexible trimmer for Illumina
576 sequence data. *Bioinformatics*, **30**, 2114-20.
577 Broman, K.W., Gatti, D.M., Simecek, P., Furlotte, N.A., Prins, P., Sen, Ś. et al. (2019) R/qtl2:
578 software for mapping quantitative trait loci with high-dimensional data and multiparent
579 populations. *Genetics*, **211**, 495-502.
580 Busi, R., Goggin, D.E., Heap, I.M., Horak, M.J., Jugulam, M., Masters, R.A. et al. (2018) Weed
581 resistance to synthetic auxin herbicides. *Pest Management Science*, **74**, 2265-2276.
582 Camacho, C., Coulouris, G., Avagyan, V., Ma, N., Papadopoulos, J., Bealer, K. et al. (2009)
583 BLAST+: architecture and applications. *BMC Bioinformatics*, **10**, 421.
584 Cheng, H., Concepcion, G.T., Feng, X., Zhang, H. & Li, H. (2021) Haplotype-resolved de novo
585 assembly using phased assembly graphs with hifiasm. *Nature Methods*, **18**, 170-175.
586 Christoffoleti, P., Figueiredo, M., Peres, L., Nissen, S. & Gaines, T. (2015) Auxinic herbicides,
587 mechanisms of action, and weed resistance: A look into recent. *Scientia Agricola*, **72**, 356-
588 362.
589 Clough, S.J. & Bent, A.F. (1998) Floral dip: a simplified method for *Agrobacterium*-mediated
590 transformation of *Arabidopsis thaliana*. *The Plant Journal*, **16**, 735-43.

591 de Figueiredo, M.R.A., Barnes, H., Boot, C.M., de Figueiredo, A., Nissen, S.J., Dayan, F.E. et al.
592 (2022a) Identification of a novel 2,4-D metabolic detoxification pathway in 2,4-D-resistant
593 waterhemp (*Amaranthus tuberculatus*). *J Agric Food Chem*, **70**, 15380-15389.
594 de Figueiredo, M.R.A., Küpper, A., Malone, J.M., Petrovic, T., de Figueiredo, A.B.T.B.,
595 Campagnola, G. et al. (2022b) An in-frame deletion mutation in the degron tail of auxin
596 coreceptor IAA2 confers resistance to the herbicide 2,4-D in *Sisymbrium orientale*.
597 *Proceedings of the National Academy of Sciences*, **119**, e2105819119.
598 Dharmasiri, N., Dharmasiri, S. & Estelle, M. (2005) The F-box protein TIR1 is an auxin receptor.
599 *Nature*, **435**, 441-5.
600 Doyle, J. & Doyle, J. (1990) A rapid total DNA preparation procedure for fresh plant tissue.
601 *Focus*, **12**, 13-15.
602 Dyer, W.E. (2018) Stress-induced evolution of herbicide resistance and related pleiotropic
603 effects. *Pest Management Science*, **74**, 1759-1768.
604 Espinosa, E., Bautista, R., Larrosa, R. & Plata, O. (2024) Advancements in long-read genome
605 sequencing technologies and algorithms. *Genomics*, **116**, 110842.
606 Ge, X., d'Avignon, D.A., Ackerman, J.J. & Sammons, R.D. (2010) Rapid vacuolar sequestration:
607 the horseweed glyphosate resistance mechanism. *Pest Manag Sci*, **66**, 345-8.
608 Ghanizadeh, H., He, L., Griffiths, A.G., Harrington, K.C., Carbone, V., Wu, H. et al. (2024) A
609 novel mutation in *IAA16* is associated with dicamba resistance in *Chenopodium album*. *Pest*
610 *Manag Sci*, 10.1002/ps.8071
611 Gleason, C., Foley, R.C. & Singh, K.B. (2011) Mutant analysis in Arabidopsis provides insight
612 into the molecular mode of action of the auxinic herbicide dicamba. *PLOS ONE*, **6**, e17245.

613 Gray, W.M., Kepinski, S., Rouse, D., Leyser, O. & Estelle, M. (2001) Auxin regulates
614 SCF(TIR1)-dependent degradation of AUX/IAA proteins. *Nature*, **414**, 271-6.
615 Grossmann, K. (2010) Auxin herbicides: current status of mechanism and mode of action. *Pest*
616 *Manag Sci*, **66**, 113-20.
617 Hall, N., Chen, J., Matzrafi, M., Saski, C.A., Westra, P., Gaines, T.A. et al. (2023) *FHY3/FAR1*
618 transposable elements generate adaptive genetic variation in the *Bassia scoparia* genome.
619 *bioRxiv*, **DOI**, 10.1101/2023.05.26.542497.
620 Heap, I., The International Herbicide-Resistant Weed Database. www.weedscience.org [accessed
621 20 June 2024].
622 Holmes, K.H., Lindquist, J.L., Rebarber, R., Werle, R., Yerka, M. & Tenhumberg, B. (2022)
623 Modeling the evolution of herbicide resistance in weed species with a complex life cycle.
624 *Ecological Applications*, **32**, e02473.
625 Kepinski, S. & Leyser, O. (2005) The Arabidopsis F-box protein TIR1 is an auxin receptor.
626 *Nature*, **435**, 446-451.
627 Kniss, A.R., Vassios, J.D., Nissen, S.J. & Ritz, C. (2011) Nonlinear regression analysis of
628 herbicide absorption studies. *Weed Science*, **59**, 601-610.
629 Kumar, S., Stecher, G., Li, M., Knyaz, C. & Tamura, K. (2018) MEGA X: Molecular
630 Evolutionary Genetics Analysis across Computing Platforms. *Mol Biol Evol*, **35**, 1547-1549.
631 LeClere, S., Wu, C., Westra, P. & Sammons, R.D. (2018) Cross-resistance to dicamba, 2,4-D,
632 and fluroxypyr in *Kochia scoparia* is endowed by a mutation in an *AUX/IAA* gene.
633 *Proceedings of the National Academy of Sciences*, **115**, E2911-E2920.
634 Li, H. & Durbin, R. (2009) Fast and accurate short read alignment with Burrows–Wheeler
635 transform. *Bioinformatics*, **25**, 1754-1760.

636 Li, H., Handsaker, B., Wysoker, A., Fennell, T., Ruan, J., Homer, N. et al. (2009) The Sequence
637 Alignment/Map format and SAMtools. *Bioinformatics*, **25**, 2078-2079.
638 Ma, Q., Grones, P. & Robert, S. (2017) Auxin signaling: a big question to be addressed by small
639 molecules. *Journal of Experimental Botany*, **69**, 313-328.
640 Martin, S.L., Benedict, L., Wei, W., Sauder, C.A., Beckie, H.J. & Hall, L.M. (2020) High gene
641 flow maintains genetic diversity following selection for high *EPSPS* copy number in the
642 weed kochia (Amaranthaceae). *Scientific Reports*, **10**, 18864.
643 McCauley, C.L., McAdam, S.A.M., Bhide, K., Thimmapuram, J., Banks, J.A. & Young, B.G.
644 (2020) Transcriptomics in Erigeron canadensis reveals rapid photosynthetic and hormonal
645 responses to auxin herbicide application. *Journal of Experimental Botany*, **71**, 3701-3709.
646 Montgomery, J., Morran, S., MacGregor, D.R., McElroy, J.S., Neve, P., Neto, C. et al. (2024)
647 Current status of community resources and priorities for weed genomics research. *Genome*
648 *Biology*, **25**, 139.
649 Nyholt, D.R. (2000) All LODs are not created equal. *Am J Hum Genet*, **67**, 282-8.
650 Ossowski, S., Schneeberger, K., Lucas-Lledó, J.I., Warthmann, N., Clark, R.M., Shaw, R.G. et al.
651 (2010) The rate and molecular spectrum of spontaneous mutations in *Arabidopsis thaliana*.
652 *Science*, **327**, 92-4.
653 Patterson, E.L., Saski, C.A., Sloan, D.B., Tranel, P.J., Westra, P. & Gaines, T.A. (2019) The draft
654 genome of *Kochia scoparia* and the mechanism of glyphosate resistance via transposon-
655 mediated *EPSPS* tandem gene duplication. *Genome Biol Evol*, **11**, 2927-2940.
656 Pettinga, D.J., Ou, J., Patterson, E.L., Jugulam, M., Westra, P. & Gaines, T.A. (2018) Increased
657 *chalcone synthase* (*CHS*) expression is associated with dicamba resistance in *Kochia*
658 *scoparia*. *Pest Management Science*, **74**, 2306-2315.

659 Poplin, R., Ruano-Rubio, V., DePristo, M.A., Fennell, T.J., Carneiro, M.O., Van der Auwera,
660 G.A. et al. (2018) Scaling accurate genetic variant discovery to tens of thousands of samples.
661 *bioRxiv*, 10.1101/201178201178.
662 Preston, C., Belles, D.S., Westra, P.H., Nissen, S.J. & Ward, S.M. (2009) Inheritance of
663 resistance to the auxinic herbicide dicamba in kochia (*Kochia scoparia*). *Weed Science*, **57**,
664 43-47.
665 Quastel, J.H. (1950) 2,4-Dichlorophenoxyacetic acid (2,4-D) as a selective herbicide. In
666 *Agricultural Control Chemicals* eds). American Chemical Society, pp. 244-249.
667 R-Core-Team, R: A Language and Environment for Statistical Computing. https://www.R-
668 project.org/ [accessed
669 Ramans-Harborough, S., Kalverda, A.P., Manfield, I.W., Thompson, G.S., Kieffer, M., Uzunova,
670 V. et al. (2023) Intrinsic disorder and conformational coexistence in auxin coreceptors. *Proc*
671 *Natl Acad Sci U S A*, **120**, e2221286120.
672 Ravet, K., Sparks, C.D., Dixon, A.L., Küpper, A., Westra, E.P., Pettinga, D.J. et al. (2021)
673 Genomic-based epidemiology reveals independent origins and gene flow of glyphosate
674 resistance in Bassia scoparia populations across North America. *Mol Ecol*, **30**, 5343-5359.
675 Ritz, C., Baty, F., Streibig, J.C. & Gerhard, D. (2015) Dose-response analysis using R. *PLOS*
676 *ONE*, **10**, e0146021.
677 Roux, F. & Reboud, X. (2005) Is the cost of herbicide resistance expressed in the breakdown of
678 the relationships between characters? A case study using synthetic-auxin-resistant
679 Arabidopsis thaliana mutants. *Genet Res*, **85**, 101-10.

680 Ruegger, M., Dewey, E., Gray, W.M., Hobbie, L., Turner, J. & Estelle, M. (1998) The TIR1
681 protein of Arabidopsis functions in auxin response and is related to human SKP2 and yeast
682 grr1p. *Genes Dev*, **12**, 198-207.
683 Song, Y. (2014) Insight into the mode of action of 2,4-dichlorophenoxyacetic acid (2,4-D) as an
684 herbicide. *Journal of Integrative Plant Biology*, **56**, 106-113.
685 Tan, X., Calderon-Villalobos, L.I., Sharon, M., Zheng, C., Robinson, C.V., Estelle, M. et al.
686 (2007) Mechanism of auxin perception by the TIR1 ubiquitin ligase. *Nature*, **446**, 640-5.
687 Tatematsu, K., Kumagai, S., Muto, H., Sato, A., Watahiki, M.K., Harper, R.M. et al. (2004)
688 MASSUGU2 encodes Aux/IAA19, an auxin-regulated protein that functions together with
689 the transcriptional activator NPH4/ARF7 to regulate differential growth responses of
690 hypocotyl and formation of lateral roots in *Arabidopsis thaliana*. *Plant Cell*, **16**, 379-93.
691 Todd, O.E., Figueiredo, M.R.A., Morran, S., Soni, N., Preston, C., Kubeš, M.F. et al. (2020)
692 Synthetic auxin herbicides: finding the lock and key to weed resistance. *Plant Sci*, **300**,
693 110631.
694 Todd, O.E., Patterson, E.L., Westra, E.P., Nissen, S.J., Araujo, A.L.S., Kramer, W.B. et al. (2024)
695 Enhanced metabolic detoxification is associated with fluroxypyr resistance in Bassia
696 scoparia. *Plant Direct*, **8**, e560.
697 Uzunova, V.V., Quareshy, M., Del Genio, C.I. & Napier, R.M. (2016) Tomographic docking
698 suggests the mechanism of auxin receptor TIR1 selectivity. *Open Biol*, **6**, 160139.
699 Van der Auwera, G. & O'Connor, B. (2020) *Genomics in the Cloud: Using Docker, GATK, and*
700 *WDL in Terra (1st Edition)*. O'Reilly Media
701 Walsh, T.A., Neal, R., Merlo, A.O., Honma, M., Hicks, G.R., Wolff, K. et al. (2006) Mutations in
702 an auxin receptor homolog *AFB5* and in *SGT1b* confer resistance to synthetic picolinate

703 auxins and not to 2,4-dichlorophenoxyacetic acid or indole-3-acetic acid in Arabidopsis.
704 *Plant Physiol*, **142**, 542-52.
705 Westra, E.P., Nissen, S.J., Getts, T.J., Westra, P. & Gaines, T.A. (2019) Survey reveals frequency
706 of multiple resistance to glyphosate and dicamba in kochia (*Bassia scoparia*). *Weed*
707 *Technology*, **33**, 664-672.
708 Wickham, H. (2016) *ggplot2: Elegant Graphics for Data Analysis*. Springer-Verlag New York
709 Wright, T.R., Shan, G., Walsh, T.A., Lira, J.M., Cui, C., Song, P. et al. (2010) Robust crop
710 resistance to broadleaf and grass herbicides provided by *aryloxyalkanoate dioxygenase*
711 transgenes. *Proc Natl Acad Sci U S A*, **107**, 20240-5.
712 Wu, C., LeClere, S., Liu, K., Paciorek, M., Perez-Jones, A., Westra, P. et al. (2021) A dicamba
713 resistance-endowing IAA16 mutation leads to significant vegetative growth defects and
714 impaired competitiveness in kochia (*Bassia scoparia*). *Pest Manag Sci*, **77**, 795-804.
715 Zenser, N., Ellsmore, A., Leasure, C. & Callis, J. (2001) Auxin Modulates the Degradation Rate
716 of Aux/IAA Proteins. *Proceedings of the National Academy of Sciences of the United States*
717 *of America*, **98**, 11795-11800.
718 Zhang, R.-G., Li, G.-Y., Wang, X.-L., Dainat, J., Wang, Z.-X., Ou, S. et al. (2022) TEsorter: An
719 accurate and fast method to classify LTR-retrotransposons in plant genomes. *Horticulture*
720 *Research*, **9**, uhac017.
721